CHEMISTRY
A EUROPEAN JOURNAL

DOI: 10.1002/chem.200600863

VIP

MTO Schiff-Base Complexes: Synthesis, Structures and Catalytic Applications in Olefin Epoxidation

Ming-Dong Zhou,[a] Jin Zhao,[b, e] Jun Li,[a] Shuang Yue,[a] Chang-Nian Bao,[a] Janos Mink,[c] Shu-Liang Zang,*[a] and Fritz E. Kühn*[b, d]

Abstract: Several Schiff-base ligands readily form complexes with methyltrioxorhenium(VII) (MTO) by undergoing a hydrogen transfer from a ligand-bound OH group to a ligand N atom. The resulting complexes are stable at room temperature and can be handled and stored in air without problems. Due to the steric demands of the ligands they display distorted trigonal-bipyramidal structures in the solid state, as shown by X-ray crystallography, with the O^- moiety binding to the Lewis acidic Re atom and the Re-bound methyl group being located either in *cis* or *trans* position to the Schiff base. In solution, however, the steric differences seem not to be maintained, as can be deduced from ^{17}O NMR spectroscopy. Furthermore, the Schiff-base ligands exchange with donor ligands. Nevertheless, the catalytic behaviour is influenced significantly by the Schiff bases coordinated to the MTO moiety, which lead either to high selectivities and good activities or to catalyst decomposition. A large excess of ligand, in contrast to the observations with aromatic N-donor ligands, is detrimental to the catalytic performance as it leads to catalyst decomposition.

Keywords: epoxidation · homogeneous catalysis · rhenium · Schiff bases · structure–activity relationships

[a] M. D. Zhou, J. Li, S. Yue, C. N. Bao, Prof. S. L. Zang
Department of Chemistry, Liaoning University, Chongshan Middle Road, No. 66, 110036 Shenyang (P.R. China)
Fax: (+86) 24-6220-2006
E-mail: slzang@lnu.edu.cn

[b] Dr. J. Zhao, Prof. Dr. F. E. Kühn
Department of Chemistry
der Technischen Universität München
Lichtenbergstrasse 4, 85747 Garching bei München (Germany)
Fax: (+49) 89-289-13473
E-mail: fekuehn@itn.pt
fritz.kuehn@ch.tum.de

[c] Prof. Dr. J. Mink
Chemical Research Centre of the Hungarian Academy of Sciences
Pusztaszeri út 59–67, 1025 Budapest (Hungary)
and
Analytical Chemistry Research Group of the Hungarian Academy of Sciences and Research Institute of Chemical and Process Engineering
University of Veszprém, Egyetem u. 10, 8200 Veszprém (Hungary)

[d] Prof. Dr. F. E. Kühn
Department of Chemistry, Instituto Tecnológico e Nuclear (ITN)
Estrada Nacional No. 10, 2686-953 Sacavém (Portugal)
Fax: (+35) 121-9946185

[e] Dr. J. Zhao
Department of Chemistry, National University of Singapore, 3 Science Drive 3, Kent Ridge, 117543 (Singapore)
and
GIST German Institute of Science and Technology Pte. Ltd.
25 International Business Park, 04-28 German Centre, 609916 (Singapore)

Introduction

Methyltrioxorhenium (MTO), which was considered as a mere curiosity when it was first described,[1] has become an almost unparalleled success story since it became available in larger amounts from improved syntheses.[2] It has been shown, mainly by the research groups of Herrmann and Espenson, that MTO is an extremely versatile catalyst or catalyst precursor for a broad variety of organic reactions.[3] Olefin epoxidation is one of the best examined of this plethora of applications,[4] and not only has one of the active species been isolated and fully characterised, including by X-ray crystallography, but the reaction mechanism has also been examined in great detail, both from a kinetic and theoretical point of view, and both homogeneous and heterogeneous variations of the reaction have been published.[5] It turns out, however, that MTO, due to its pronounced Lewis acidity, has a tendency to promote further ring-opening reactions of the epoxidation products to give diols.[6] It was recognised quite early that the presence of Lewis bases, for example nitrogen donor ligands, suppresses such unwanted side reactions.[7] Nevertheless, the activity of MTO–Lewis base adducts was originally found to be significantly lower than that of MTO itself.[8] The use of aromatic N-donor ligands in significant excess (ca. 10–12:1) together with MTO,

however, leads to higher activities and selectivities in epoxidation catalysis than with MTO alone.[9] Both mono- and didentate aromatic Lewis bases with N-donor ligands display this behaviour.[10] In the meantime, many N-ligand adducts of MTO have been isolated, characterised and applied for the epoxidation of olefins as catalysts.[11] Other donor adducts of MTO, despite being mentioned sporadically in the literature, have never been examined to the same extent with respect to their applicability as epoxidation catalysts.[12]

Rhenium complexes with Schiff-base ligands derived from salicylaldehyde and mono- or diamines have received attention due to their applications in catalysis and nuclear medicine. However, to the best of our knowledge, only Re^{V} oxo complexes bearing Schiff-base ligands have been investigated extensively so far,[13] and Schiff-base adducts of MTO have not been described and applied as epoxidation catalysts until now. Herein we present the synthesis and molecular structure of a series of MTO adducts containing Schiff-base ligands and their application in the epoxidation of olefins.

Results and Discussion

Synthesis and spectroscopic characterisation: Compounds **1**–**5** (see Scheme 1) were easily synthesised by treating MTO with donor ligands in diethyl ether at room temperature. All

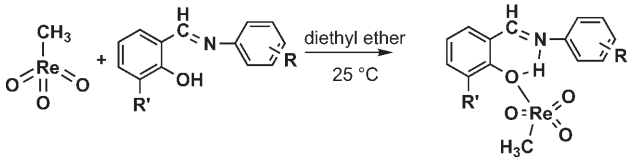

R'= H,R= H (**1**); R'= H, R= *p*-CH_3 (**2**); R'= H, R= *p*-Cl (**3**);
R'= H, R= *p*-OCH_3 (**4**); R'= -OCH_3;R= *p*-CH_3 (**5**)

Scheme 1. Synthesis of MTO adducts containing Schiff-base ligands.

products were isolated as orange (**1**–**4**) or red (**5**) crystals in yields higher than 80%. In comparison to many N-coordinated Lewis base adducts, which are considerably more sensitive to the presence of moisture and temperature than MTO itself,[9e,10a,b,14,15] compounds **1**–**5** show good stability at room temperature both in the solid state and in solution. They can be handled in a normal laboratory atmosphere and stored under air without any decomposition.

The Re=O vibrations in the IR spectra of compounds **1**–**5** are found in the region 910–1080 cm^{-1}. The asymmetric ReO_3 stretching bands show a splitting of 10–30 cm^{-1} due to the complex symmetry (see Table 1). Compared to the vibrations of non-coordinated MTO (see averaged values of the Re=O stretches), the Re=O bands of compounds **1**–**5** are strongly red-shifted due to the pronounced donor capacity of the respective ligands in the solid state. The additional electron density donated from the ligand to the rhenium(VII) centre generally reduces the bond order of

Table 1. Characteristic vibrations of the $(CH_3)ReO_3$ fragments (cm^{-1}) in **1**–**5**.

MTO[10d]	**1**	**2**	**3**	**4**	**5**	Assignment
1368	1376	1375	1375	1380	1375	CH_3 asym. def.
1205	1216	1210	1215	–	–	CH_3 sym. def.
998	1005	1007	1012	1035	1080	ReO_3 sym. str.
965	928	935	950	925	925	ReO_3 asym. str.
	919	911	921	914	913	
567	576	576	573	525	585	ReC str.
976	950	951	961	958	973	ReO str. average
33	81.5	84	76.5	120.5	166	(ν_s–ν_a) ReO_3

the Re=O bonds. This is clearly true for complexes **1**–**3**, although the situation is somewhat different for derivatives **4** and **5**. For the latter compounds one Re=O bond is more strongly enhanced whereas the other two are slightly weakened. Accordingly, the so-called ReO symmetric stretching bands are observed at 1035 and 1080 cm^{-1} for complexes **4** and **5**, respectively. Another difference in the coordination of MTO in the two different types of complexes (**1**–**3** versus **4**, **5**) can be clearly seen from the difference between the averaged symmetric and asymmetric stretching vibrations of the ReO_3 moiety (last row in Table 1). For free MTO this difference is only 33 cm^{-1} (tetrahedral coordination), for complexes **1**–**3** it is around 80 cm^{-1} (trigonal-bipyramidal coordination) and it is very large for complexes **4** (121 cm^{-1}) and **5** (167 cm^{-1}) due to the rather asymmetric coordination of the rhenium(VII) atom.

The absence of OH stretching bands of the Schiff bases in the region around 3400 cm^{-1} indicates the presence of a strong intramolecular hydrogen bond with the nitrogen atom of the imine group to form a six-membered ring. The broad band with a specific fine structure in the range 2900–2400 cm^{-1} is most likely due to the phenolic OH stretching feature characteristic of a strong hydrogen bond. There are other low frequency bands characteristic for a phenolic OH group in the spectra of the pure Schiff-base ligands. These bands, together with the OH stretches, are conspicuously absent in the spectra of compounds **1**–**5** (see Table 2), thereby indicating that the proton changes its location during the coordination with MTO. These observations provide strong evidence that the phenolic OH proton is lost from the oxygen during coordination. In the case of the Schiff base $C_{15}H_{15}NO_2$ (corresponding to complex **5**), the phenolic ring substitution is different from the others (2,6-substitution), therefore the phenolic OH group and coupled ring vibrations are slightly different.

As a rule, PhCH=NPh type molecules have a medium/strong band at 1650 cm^{-1} for the C=N stretching mode in an undisturbed situation. In the case of the free ligands of complexes **1**–**5** strong bands are observed, however, at 1611–1622 cm^{-1} (see Table 2). This frequency lowering of 40–30 cm^{-1} can be explained by the existence of an intramolecular hydrogen bond between the phenolic hydrogen and the nitrogen atom. After complexation to MTO the proton becomes attached to the nitrogen to form an imine group C=

Table 2. Selected IR (KBr) data [cm^{-1}] for $C_{13}H_{11}NO$ and compounds **1–5**. The respective pure ligand vibrations are given for sake of comparison.

Compound	Imine group	Phenolic OH group and coupled ring vibrations				
	$\nu_{(C=N)}$	β(NH···O)	$\nu_{(CX)}$	$\nu_{(CX)}$	$\nu_{(CX)}$	γ(OH)
$C_{13}H_{11}NO$	1616 s	1358 m	1275 vs	1074 m	871 vs	734 w,m[a]
$C_{13}H_{11}NO{\cdot}(CH_3)ReO_3$ (**1**)	1643 s					
$C_{14}H_{13}NO$	1616 s	1358 m	1275	1074 m	845 m,sh	730 m,sh[a]
$C_{14}H_{13}NO{\cdot}(CH_3)ReO_3$ (**2**)	1645 s					
$C_{13}H_{10}ClNO$	1622 s	1360 m	1281 vs	1031 m,sh	838 m	740 m,sh[a]
$C_{13}H_{10}ClNO{\cdot}(CH_3)ReO_3$ (**3**)	1643 s					
$C_{14}H_{13}NO_2$	1617 s	1346 m	1217 m	1080 s	866 s	736 vs[a]
$C_{14}H_{13}NO_2{\cdot}(CH_3)ReO_3$ (**4**)	1637 s					
$C_{15}H_{15}NO_2$	1611 s	1396 m	1272 s	1150 m	816 m	698 m[b]
$C_{15}H_{15}NO_2{\cdot}(CH_3)ReO_3$ (**5**)	1638 s					

[a] Characteristic bands of *ortho*-substituted phenols. [b] Characteristic bands of 2,6-disubstituted phenols. Notation of vibrational modes: ν(C=N): C=N stretching; β(OH···O): hydrogen-bonded OH in-plane deformation; ν(CX) substituent-sensitive aromatic ring stretches; γ(OH) phenolic out-of-plane vibrations.

N^+(-H), the C=N^+ stretching frequency of which is accordingly found at higher wavenumbers (1637–1645 cm^{-1}).

The ^1H and ^{13}C NMR spectroscopic data of the $ReCH_3$ groups of compounds **1–5** are shown in Table 3. In the ^1H NMR spectra, the proton signals originating from the

Table 3. Selected ^1H and ^{13}C NMR spectroscopic data for the MTO complexes in $CDCl_3$.

Compound	MTO-CH_3	
	$\delta(^1H)$	$\delta(^{13}C)$
MTO	2.67	19.03
1	2.62	19.43
2	2.63	19.61
3	2.62	19.40
4	2.61	19.73
5	2.58	19.40

$ReCH_3$ group of compounds **1–5** are shifted to high field with respect to that of MTO. Similarly, a small ^{13}C NMR shift change for the Re-bound carbon atom of the methyl group in compounds **1–5** can be observed, thus revealing that the Schiff-base ligands in compounds **1–5** have a comparatively weak influence on the $ReCH_3$ moiety in solution. It is noteworthy that several monodentate N-ligand adducts show a stronger shift difference relative to non-coordinated MTO than is observed for complexes **1–5** in both their ^1H and ^{13}C NMR spectra. For example, the chemical shift change in the ^1H NMR spectrum is about 0.5–0.9 ppm for pyridine derivatives of MTO, and in the ^{13}C NMR spectra it is around 4–6 ppm (in $CDCl_3$).[10a] N-oxide adducts of MTO also show larger chemical shift changes in both the ^1H and ^{13}C NMR spectra than the compounds described here.[12] The proton signals of the OH groups appear at around $\delta =$ 13 ppm in the free ligand. After reaction with MTO, however, the peaks are significantly broadened in all cases, thereby indicating a higher mobility of the proton. The ^1H and ^{13}C NMR signals of the imine group of compounds **1–5** are shifted to slightly lower field, in agreement with a changed coordination situation.

Only the peaks of the Schiff-base ligands can be observed in all cases in the FAB mass spectra, whereas the CI mass spectra of compounds **1–5** show the peaks of the Schiff-base ligand and the MTO moiety separately, although no molecular peak of the complete molecules can be observed.

The thermal stability of complexes **1–5** was examined by thermogravimetric analysis (TGA) coupled with mass spectrometry (MS) between 20 and 1000 °C. The thermal decomposition behaviour of complexes **1–4** is rather similar. The onset temperatures for the first decomposition step are around 108, 108, 107 and 97 °C and the onset temperatures for the second decomposition step are around 408, 396, 471 and 407 °C, respectively. The mass loss for these two steps is in agreement with the mass of the Schiff-base ligand. The phenyl ring is lost after the first decomposition onset, followed by the loss of the imine and the phenolic ring after the second onset. In the case of complexes **1**, **3** and **4**, no further mass loss is observed between 600 and 1000 °C. However, in the case of complex **2**, a further decomposition step associated with a mass loss of 14 % can be observed. The onset temperature of this third decomposition step is about 680 °C. This step ends at about 800 °C, the remaining mass being equivalent to the Re content of compound **1**. Complex **5** starts decomposing at about 77 °C and in one large step loses 62 % of the original mass up to 600 °C. The observed mass loss is consistent with the total mass of the Schiff-base ligand, the three oxygens and the methyl ligand. Similarly to complex **2**, above 800 °C only rhenium metal remains (EA evidence). The presence of a Schiff-base ligand changes the behaviour of the MTO moiety completely under TGA conditions.[16]

X-ray crystal structures of compounds 1–5: The solid-state structures of the examined compounds are shown below, with selected bond lengths listed in Table 4 and bond angles in Table 5 for **1–3** and Table 6 for **4** and **5**. All five compounds display a distorted trigonal-bipyramidal geometry. As is known for most structurally characterised intermolecular N- and O-donor adducts of MTO,[6,10] the ReO_3 fragment is located in the equatorial plane in the case of complexes **1–3** (Figures 1, 2 and 3, respectively), while the methyl group and the donating oxygen function of the Schiff-base ligands reside in the apical sites in the *trans* position. However, in complexes **4** (Figure 4) and **5** (Figure 5), the methyl group and two oxo ligands occupy the equatorial positions while the donating phenolic group and the remaining oxo ligand occupy the axial positions. Very few MTO adducts with such an arrangement of the ReO_3 moiety have been reported to date.[3,6] With the exception of some intermolecu-

Table 4. Selected bond lengths [Å] for compounds **1**–**5**.

Compound	**1**	**2**	**3**	**4**	**5**
Re(1)–O(2)	1.699(6)	1.702(4)	1.700(5)		
Re(1)–O(3)	1.675(7)	1.694(5)	1.697(6)	1.699(6)	1.702(8)
Re(1)–O(4)				1.710(5)	1.698(8)
Re(1)–O(5)				1.701(5)	1.690(9)
Re(1)–O(2)#1[a]	1.699(6)	1.702(4)	1.700(5)		
Re(1)–C(14)	2.112(12)		2.095(11)		
Re(1)–C(15)		2.084(8)		2.119(7)	
Re(1)–C(16)					2.089(12)
Re(1)–O(1)	2.269(7)	2.243(4)	2.286(5)	2.153(5)	2.210(7)
O(1)–C(3)	1.317(11)	1.309(7)	1.305(9)	1.325(8)	1.303(11)
N(1)–C(1)	1.304(12)	1.292(8)	1.302(9)	1.314(8)	1.300(13)
N(1)–H(1 A)	1.00(14)	0.8600	0.77(9)	0.89(7)	0.86(12)

[a] Symmetry transformations used to generate equivalent atoms: #1: x, $-y+1/2$, z.

Table 5. Selected bond angles [°] for compounds **1**–**3**.

1[a]		**2**[b]		**3**[c]	
O(3)–Re(1)-O(2)#1	119.7(3)	O(3)-Re(1)-O(2)	119.41(14)	O(3)-Re(1)-O(2)	118.99(18)
O(3)-Re(1)-O(2)	119.7(3)	O(3)-Re(1)-O(2)#1	119.41(14)	O(3)-Re(1)-O(2)#1	118.99(18)
O(2)#1-Re(1)-O(2)	117.9(5)	O(2)-Re(1)-O(2)#1	118.9(3)	O(2)-Re(1)-O(2)#1	119.2(4)
O(3)-Re(1)-C(14)	95.9(5)	O(3)-Re(1)-C(15)	94.4(4)	O(3)-Re(1)-C(14)	96.8(5)
O(2)#1-Re(1)-C(14)	95.2(3)	O(2)-Re(1)-C(15)	95.27(19)	O(2)-Re(1)-C(14)	95.0(3)
O(2)-Re(1)-C(14)	95.2(3)	O(2)#1-Re(1)-C(15)	95.27(19)	O(2)#1-Re(1)-C(14)	95.0(3)
O(3)-Re(1)-O(1)	80.8(3)	O(3)-Re(1)-O(1)	80.6(2)	O(3)-Re(1)-O(1)	81.0(3)
O(2)#1-Re(1)-O(1)	86.5(2)	O(2)-Re(1)-O(1)	87.23(14)	O(2)-Re(1)-O(1)	86.14(16)
O(2)-Re(1)-O(1)	86.5(2)	O(2)#1-Re(1)-O(1)	87.23(14)	O(2)#1-Re(1)-O(1)	86.14(16)
C(14)-Re(1)-O(1)	176.6(4)	C(15)-Re(1)-O(1)	175.0(3)	C(14)-Re(1)-O(1)	177.8(4)
C(3)-O(1)-Re(1)	130.6(6)	C(3)-O(1)-Re(1)	131.5(4)	C(3)-O(1)-Re(1)	130.7(4)

[a] Symmetry transformations used to generate equivalent atoms: #1: x, $-y+1/2$, z. [b] Symmetry transformations used to generate equivalent atoms: #1: x, $-y+3/2$, z. [c] Symmetry transformations used to generate equivalent atoms: #1: x, $-y+3/2$, z.

Table 6. Selected bond angles [°] for compounds **4** and **5**.

4		**5**	
O(3)-Re(1)-O(5)	104.2(3)	O(5)-Re(1)-O(4)	104.5(5)
O(3)-Re(1)-O(4)	118.9(3)	O(5)-Re(1)-O(3)	103.8(5)
O(5)-Re(1)-O(4)	103.3(3)	O(4)-Re(1)-O(3)	118.0(4)
O(3)-Re(1)-C(15)	116.0(3)	O(5)-Re(1)-C(16)	89.1(5)
O(5)-Re(1)-C(15)	87.4(3)	O(4)-Re(1)-C(16)	112.7(6)
O(4)-Re(1)-C(15)	118.8(3)	O(3)-Re(1)-C(16)	121.7(5)
O(3)-Re(1)-O(1)	80.9(2)	O(5)-Re(1)-O(1)	167.5(4)
O(5)-Re(1)-O(1)	167.0(2)	O(4)-Re(1)-O(1)	80.0(3)
O(4)-Re(1)-O(1)	84.1(2)	O(3)-Re(1)-O(1)	83.8(4)
C(15)-Re(1)-O(1)	79.7(3)	C(16)-Re(1)-O(1)	78.4(4)
C(3)-O(1)-Re(1)	135.6(4)	C(3)-O(1)-Re(1)	133.8(7)

lar donor adducts, which can only coordinate through their N- or O-donor atoms in the axial position (*cis* to the methyl group) due to steric reasons,[3,6,7,17] only one *cis*-coordinating Lewis base adduct of MTO has been described in the literature, to the best of our knowledge, along with its X-ray crystal structure. For this $[(CH_3)ReO_3(C_6H_5NH_2)]$ complex, however, a second modification exists with all the oxo ligands in the equatorial plane. This compound, too, is known from its X-ray crystal structure.[7] Packing effects have been thought to be responsible for the coordination modes observed (*cis* or *trans* with respect to the methyl group). Such an explanation may also hold for the structural differences observed for compounds **1**–**5**. The ReO_3 fragment has pseudo-tetrahedral geometry, with the O=Re=O angles varying from 103.3(3)° to 118.9(3)° in complex **4** and from 103.8(5)° to 118.0(4)° in complex **5**. The Re–C distance in compounds **1**–**5** is 2.112(12), 2.084(8), 2.095(11), 2.119(7) and 2.089(12) Å, respectively, and is slightly longer than that in free MTO (2.063(2) Å) in all cases but close to the average Re–C distance (2.09 Å) found in other N-[6] or O-donor adducts of MTO.[12] The Re=O bond lengths in complexes **1**–**5** are around 1.7 Å and are therefore quite similar to those in other MTO adducts. The Re–O bond distances are 2.269(7), 2.243(4), 2.286(5), 2.153(5) and 2.210(7) Å in complexes **1**–**5**, respectively, and are therefore significantly shorter than the average Re–N bond distance in N-donor adducts of organorhenium(VII) oxides (2.42 Å,[6]) and also notably shorter than the Re–O bond distance in some known organorhenium(VII) oxygen donor complexes, for example in 4-*tert*-butylpyridine N-oxide adducts of MTO (2.311(4) Å),[12] $[(CH_3)ReO_3\cdot\{ORe(O)(PPh_3)_2(CH_3)\}]$ (2.377(7) Å)[18]) and $C_6H_5ReO_3\cdot THF$ (2.420(2) Å),[19]) or the related distance in trioxorhenium(VII) alkoxide complexes,[17] namely the alkoxy alcohol complex $[ReO_3(OCMe_2CMe_2OH)]$ (2.323(5) Å) and the alkoxy ether complex $[ReO_3(OCMe_2CMe_2OMe)]$ (2.302(5) Å). The shorter Re–O bonds in compounds **1**–**5** are in agreement

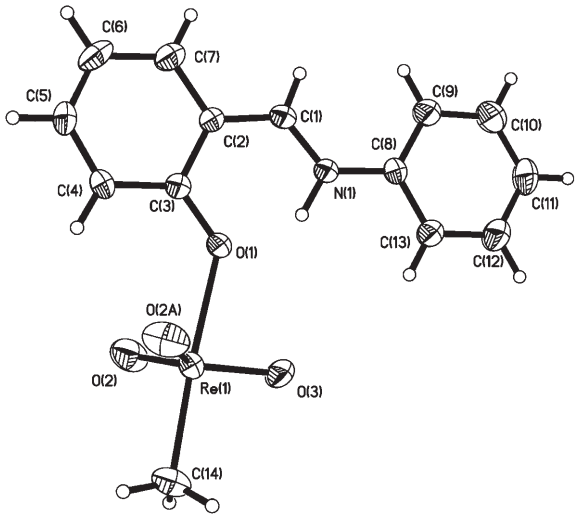

Figure 1. PLATON view of the solid-state structure of complex **1**. The thermal ellipsoids are shown at the 50% probability level. Hydrogen atoms are placed in calculated positions.

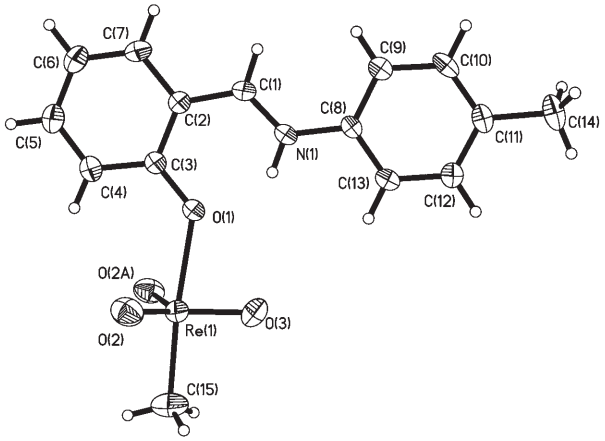

Figure 2. PLATON view of the solid-state structure of complex **2**. The thermal ellipsoids are shown at the 50% probability level. Hydrogen atoms are placed in calculated positions.

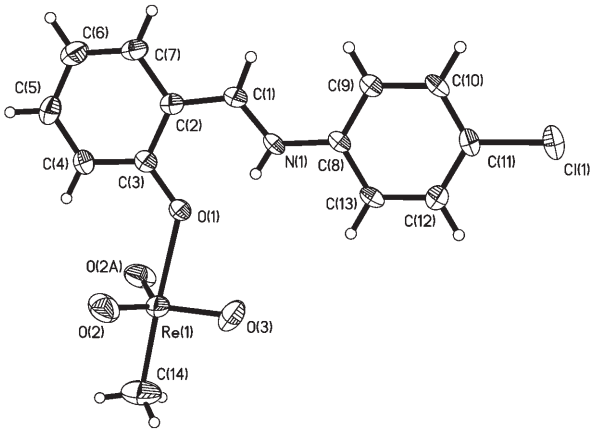

Figure 3. PLATON view of the solid-state structure of complex **3**. The thermal ellipsoids are shown at the 50% probability level. Hydrogen atoms are placed in calculated positions.

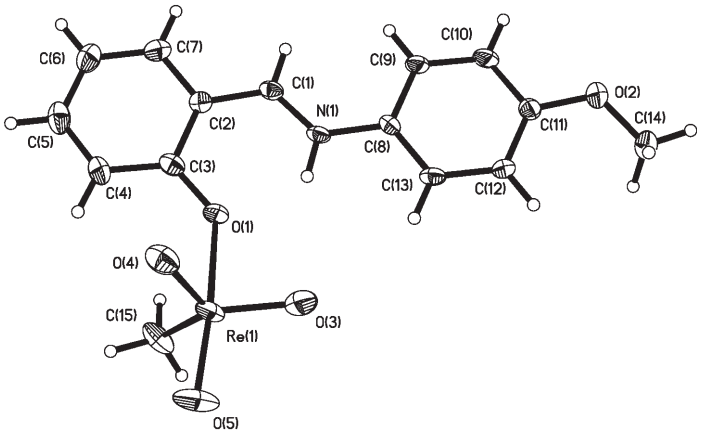

Figure 4. PLATON view of the solid-state structure of complex **4**. The thermal ellipsoids are shown at the 50% probability level. Hydrogen atoms are placed in calculated positions.

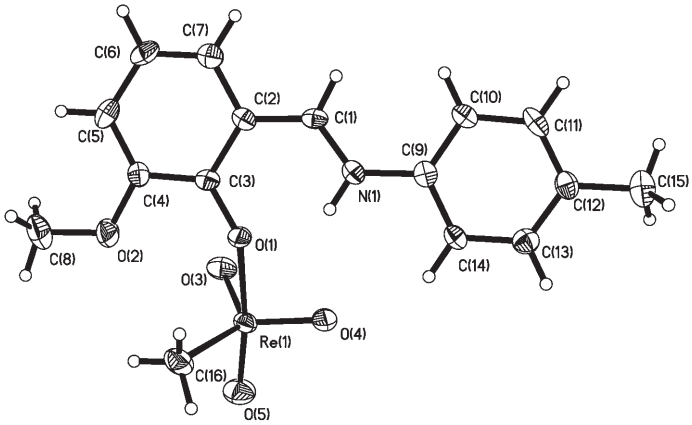

Figure 5. PLATON view of the solid-state structure of complex **5**. The thermal ellipsoids are shown at the 50% probability level. Hydrogen atoms are placed in calculated positions.

with the IR results (see above) and also indicate a movement of the originally O-bound proton to the -N=C- moiety to create a zwitterionic structure with the negatively charged oxygen atom binding to the Lewis acidic rhenium(VII) centre. It is also interesting to note that the Re–O bond length in complexes **5** and, particularly, **4** is shorter than in complexes **1**–**3**. The obtained structures also indicate that the former OH proton of the ligands is now riding on the nitrogen in complexes **1**–**5**. An intramolecular hydrogen bond between the donating oxygen atom and the hydrogen atom riding on the imine N atom seems possible. The short N(1)–O(1) bond lengths of 2.587(11), 2.578(6), 2.588(7), 2.579(7) and 2.603(11) Å, respectively, also support this assumption.

^{17}O NMR spectroscopy: The different structural features of complexes **1**–**3** (*trans* arrangement of the $ReCH_3$ group and the Schiff-base ligand) and **4** and **5** (*cis* arrangement of the $ReCH_3$ group and the Schiff-base ligand) may be due to packing effects in the solid state, as mentioned in the previous section. Therefore, it seemed interesting to examine whether the *cis* and *trans* arrangements of the respective ligands are maintained in solution. A *cis* arrangement would lead to two sets of oxygen signals (in a two to one ratio of equatorial and axial oxygens) in the ^{17}O NMR spectra, as described previously in the literature.[10,20] Usually, however, such arrangements can only be observed at low temperatures since a fast equilibrium between "axial" and "equatorial" oxygens is observed at elevated temperatures. It has been shown by labelling experiments that this interchange is due to an opening and closing of the donor ligand for both N-[8c,20] and O-donor ligands.[12,20] Both complexes **3** and **5** were examined in the temperature interval from −50 to +50 °C. Both complexes display only one ^{17}O NMR signal over the whole temperature interval, thus indicating a *trans* arrangement of the Schiff-base ligand and the Re-bound methyl group. Interestingly, the ^{17}O chemical shifts of both complexes are identical within the measurement error (see Table 7). Mixing complex **3** with the ligand of complex **5**

Table 7. Temperature-dependent ^{17}O NMR spectroscopic data for complexes **3** and **5** as well as the ligand-exchange reactions between complexes **3** and **5** and Schiff-base ligands and pyridine in $CDCl_3$.

Temp. [°C]	**3**		**5**		**3**+L5 (1:1)		**5**+L3 (1:1)		**3**+pyridine (1:1)		**5**+pyridine (1:1)	
	δ [ppm]	$\Delta\nu_{1/2}$ [Hz]	δ [ppm]	$\Delta\nu_{1/2}$ [Hz]	δ [ppm]	$\Delta\nu_{1/2}$ [Hz]	δ [ppm]	$\Delta\nu_{1/2}$ [Hz]	δ [ppm]	$\Delta\nu_{1/2}$ [Hz]	δ [ppm]	$\Delta\nu_{1/2}$ [Hz]
−50	835	116	836	122	834	157	835	203	883	400	883	425
−25	832	70	833	78	832	93	832	85	884	255	884	259
0	830	39	830	41	830	42	830	42	885	119	884	118
25	830	30	830	31	829	31	829	32	880	99	878	98
50	830	28	830	28	829	27	830	27	870	56	868	83

and vice versa leads only to a minor line broadening rather than to a significant shift change. The observed line broadening at lower temperatures is well within the normal limits and is not indicative of changes in the geometry of the complexes.[8c,12,20] Whether it indicates ligand exchange is not clear from these experiments alone since the ^{17}O signals of compounds **3** and **5** would be close together anyway. Therefore, we added pyridine to both complexes **3** and **5**. In this case a major chemical shift change towards the signal of an MTO–pyridine adduct is observed along with a more severe line broadening. These latter observations clearly point to a ligand exchange. Again, only one ^{17}O NMR signal is observed over the whole temperature range, thus indicating a *trans* positioning of the ligand, as is known for monodentate pyridine complexes.[8c,10,20]

Application in epoxidation catalysis: Compounds **1–5** were examined as catalysts for the epoxidation of cyclooctene with hydrogen peroxide. Further details of the catalytic reaction are given in the Experimental Section. Blank reactions showed that no significant amounts of epoxide are formed in the absence of catalyst. A catalyst:oxidant:substrate ratio of 1:200:100 was used in all experiments, unless stated otherwise. No significant formation of by-products (e.g. diol) was observed for cyclooctene. All catalytic reactions show similar time-dependent curves in which the yield increases steadily during the first two hours of the reaction and then slows down (first-order kinetics, as observed for related oxidizing systems;[3,10,15] see also Figure 6).

Complexes **1–3** show a similar high catalytic activity for the epoxidation of cyclooctene during the first four hours of the reaction and after 24 h the epoxide yield reaches 100%. However, the catalytic activity of complexes **4** and **5**, both of which possess an OCH_3 moiety on the phenyl ring, is relatively low, and even after a further 20 h the epoxide yield does not increase significantly compared to the yield after four hours (see Figure 7). In the reaction systems containing complexes **4** or **5**, the colour of the organic phase gradually turns from the original yellow to brownish red during the catalytic reaction, which is a strong indication of decomposition.[7] The colour change of the system with compound **5** takes place even earlier than that of the system with compound **4**, thus indicating that the catalysts decompose under these reaction conditions even during the first two hours of the reaction (see also Figure 6). In contrast, in the case of compounds **1–3** the organic phase remains yellow during the

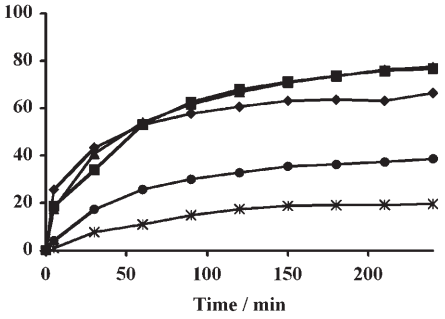

Figure 6. Time-dependent yield of cyclooctene epoxide in the presence of 1 mol% of compounds **1** (diamonds), **2** (squares), **3** (triangles), **4** (circles) or **5** (stars) as catalyst at room temperature.

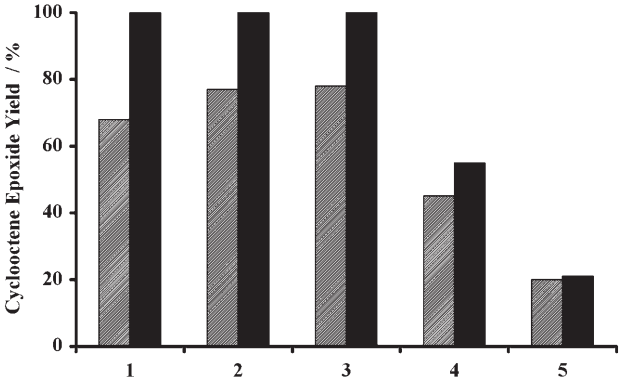

Figure 7. Yield of the cyclooctene epoxidation after 4 h (hatched bars) and after 24 h (black bars) in the presence of complexes **1–5** as catalysts.

whole 24 h reaction time. This is similar to the observations made with several aromatic N-ligated MTO complexes, which are usually quite stable under oxidative conditions.[10]

In the presence of excess H_2O_2, MTO is known to form a catalytically active bisperoxo complex of composition $[(CH_3)ReO(O_2)_2L]$ ($L = H_2O$, N-ligand, etc.) via a monoperoxo complex.[4] This latter—$[(CH_3)ReO_2(O_2)]$—is also a catalyst for the same reaction. In order to examine the different catalytic behaviour of complexes **1–3** in comparison to that of complexes **4** and **5**, kinetic ^1H NMR measurements were performed to detect the monoperoxo- and bisperoxorhenium species of complexes **1–5** in the presence of H_2O_2. Thus, H_2O_2 was gradually added to a $CDCl_3$ solution of complexes **3** and **5**, separately, as examples of the complexes

with two different Lewis base ligand configurations (see above). In the case of complex **3**, the formation of a monoperoxo complex is observed when a 1:1 ratio of MTO and H_2O_2 is used. The corresponding ^1H NMR signal is found at $\delta = 2.84$ ppm. A large excess of H_2O_2 (10 equivalents) leads to the formation of a signal at $\delta = 2.89$ ppm, which originates from a bisperoxo complex.[4,10,21] In the case of complex **5**, after the addition of one equivalent of H_2O_2 the same spectral changes are observed as in the case of complex **3**, with the signal of the monoperoxo complex occurring at $\delta =$ 2.83 ppm. However, when 10 equivalents of H_2O_2 are added no signal assignable to a bisperoxo complex is found. Instead, a pronounced methanol signal (at around $\delta =$ 3.44 ppm) appears, which indicates complex decomposition. This decomposition is also evident from the deep red colour of the reaction mixture. The formation of considerable amounts of methanol in the presence of excess H_2O_2 indicates that the Schiff-base ligands of complexes **4** and **5** promote the decomposition of MTO under catalytic conditions. These observations explain why complexes **4** and **5** show much lower catalytic activity than compounds **1**–**3** and why longer reaction times lead to no significant improvement of epoxide yield in the cases of compounds **4** and **5**.

Since the rate-accelerating effect of excess of some Lewis base ligands in the presence of MTO is known,[9,10] we examined the influence of the amount of applied ligand on the catalytic performance in olefin epoxidation with complex **3** as catalyst. When a mixture of MTO and Schiff base is used in a 1:1 ratio, a similar catalytic activity and selectivity are obtained as with complex **3**. When applying a 10:1 ratio of ligand and MTO, however, after four hours only a 32% epoxide yield is reached and after 24 h no further increase of the yield is observed. During this catalytic reaction the colour of the reaction mixture changes from yellow to deep red, as noted in the cases of compounds **4** and **5**, thus indicating that an excess of Schiff-base ligand furthers catalyst decomposition.

When complex **3** is used as catalyst for the epoxidation of 1-octene, the epoxide yield reaches 62% after four hours and 98% after 24 h, with very good selectivity (>95%). For the epoxidation of styrene the epoxide yield after 24 h is 35% and the selectivity of the reaction is higher than 80%. These results can be regarded as acceptable, particularly when compared with other epoxidation catalysts based either on rhenium or other transition metals.[3,22,23]

Conclusions

Several Schiff bases readily form stable complexes with MTO with distorted trigonal-bipyramidal structures. The Schiff-base ligands are either arranged in a *cis* or a *trans* fashion to the Re-bound methyl moiety. The phenolic proton of the ligand is transferred to a ligand imine group upon coordination to Re, which means that the Lewis acidic rhenium(VII) is coordinated to O^- and forms a comparatively short Re–O bond. In solution, the molecules seem to be flexible with respect to their structures. Nevertheless, different Schiff-base ligands have a pronounced influence on the catalytic performance of the complexes. Thus, whilst OCH_3 groups on the Schiff base seem to destabilize the resulting complex under oxidative conditions, other Schiff bases lead to active and highly selective epoxidation catalysts. An excess of ligand, however, always leads to rapid decomposition of the catalyst.

Given the ready availability and stability of the title complexes, together with the good catalytic activity and high selectivity of some of them, they appear to be good alternatives to less stable MTO N-donor complexes as epoxidation catalysts. The Schiff base adducts of the latter can also be prepared and applied in situ. In contrast to N-donor adducts, no pronounced ligand excess is necessary to achieve high yields and selectivities in olefin epoxidation catalysis.

Experimental Section

Synthesis and characterisation: All preparations and manipulations were initially performed using standard Schlenk techniques under an argon atmosphere. However, it turned out that the syntheses can also be performed under (dry) air, without problems. Solvents were dried by standard procedures (*n*-hexane and Et_2O over Na/benzophenone; CH_2Cl_2 over CaH_2), distilled under argon and used immediately or kept over 4-Å molecular sieves. Elemental analyses were performed with a Flash EA 1112 series elemental analyser. ^1H, ^{13}C NMR and ^{17}O NMR were measured in $CDCl_3$ with a mercury-VX 300 spectrometer or a 400 MHz Bruker Avance DPX-400 spectrometer. IR spectra were recorded with a Perkin Elmer FT-IR spectrometer using KBr as the IR matrix. FAB mass spectra (FAB matrix: 3-nitrobenzyl alcohol) and CI mass spectra (isobutene as CI gas) were obtained with a Finnigan MAT 90 mass spectrometer. Thermogravimetry coupled with mass spectrometry (TG-MS) was conducted utilizing a Netzsch TG209 system; typically, about 10 mg of each sample was heated from 35 to 1000 °C at 10 °C min^{-1}. Catalytic runs were monitored by GC methods on a Hewlett–Packard instrument (HP 5890 Series II) equipped with a FID, a Supelco column Alphadex 120 and a Hewlett–Packard integration unit (HP 3396 Series II). The Schiff-base ligands were prepared as described previously.[23]

Compounds **1**–**5** were prepared as follows: A solution of $[(CH_3)ReO_3]$ (0.2 g, 0.8 mmol) in diethyl ether (5 mL) was added dropwise to an equally concentrated solution of ligand (0.8 mmol) in diethyl ether (5 mL) whilst stirring at room temperature. After 15 min the yellow solution was concentrated to about 3 mL under an oil pump vacuum and the orange (**1**–**4**) or orange-red (**5**) precipitate was collected by filtration, washed with *n*-hexane and dried under reduced pressure.

1: Yield: 83%. ^1H NMR (300 MHz, $CDCl_3$, 25 °C, TMS): $\delta = 13.25$ (s, 1H; NH), 8.63 (s, 1H; CH=N), 7.46–7.26 (m, 7H; Ph), 7.05–6.92 (m, 2H; Ph), 2.62 ppm (s, 3H; MTO-CH_3); ^{13}C NMR (100.28 MHz, $CDCl_3$, 25 °C): $\delta = 162.50$ (CH=N), 161.23, 148.17, 133.16, 132.25, 129.34, 128.97, 126.87, 121.07, 119.09, 118.98, 117.24 (aryl-C), 19.43 ppm (MTO-CH_3); IR (KBr): see Tables 1 and 2; MS (FAB): *m*/*z* (%) 197.9 (100) [M^+–MTO]; elemental analysis calcd (%) for $C_{14}H_{14}NO_4Re$ (446.46): C 37.66, H 3.14, N 3.14; found: C 37.64, H 3.14, N 3.15.

2: Yield: 85%. ^1H NMR (300 MHz, $CDCl_3$, 25 °C, TMS): $\delta = 13.39$ (s, 1H; NH), 8.63 (s, 1H; CH=N), 7.40–7.38 (m, 2H; Ph), 7.21 (m, 4H; Ph), 7.05–6.94 (m, 2H; Ph), 2.63 (s, 3H; MTO-CH_3), 2.39 ppm (s, 3H; CH_3); ^{13}C NMR (100.28 MHz, $CDCl_3$, 25 °C): $\delta = 161.36$ (CH=N), 145.19, 136.92, 133.02, 132.12, 129.92, 120.82, 119.04, 118.84, 117.22 (aryl-C), 20.94 (Ph-CH_3), 19.61 ppm (MTO-CH_3); IR (KBr): see Tables 1 and 2; MS (FAB): *m*/*z* (%) 211.9 (100) [M^+–MTO]; elemental analysis calcd (%) for $C_{15}H_{16}NO_4Re$ (460.49): C 39.13, H 3.48, N 3.04; found: C 39.15, H 3.48, N 3.03.

3: Yield: 80%. ^{1}H NMR (300 MHz, $CDCl_3$, 25°C, TMS): $\delta = 13.00$ (s, 1H; NH), 8.59 (s, 1H; CH=N), 7.41–7.37 (m, 4H; Ph), 7.23- 7.20 (m, 2H; Ph), 7.04–6.92 (m, 2H; Ph), 2.62 ppm (s, 3H; MTO-CH_3); ^{13}C NMR ($CDCl_3$, 100.28 MHz, room temp.): $\delta = 162.65$ (CH=N), 161.03, 146.68, 133.35, 132.32, 129.37, 122.32, 119.07, 118.85, 117.17 (aryl-C), 19.40 ppm (MTO-CH_3); IR (KBr): see Tables 1 and 2; MS (FAB): *m*/*z* (%) 231.9 (100) [M^+−MTO]; elemental analysis calcd (%) for $C_{14}H_{13}ClNO_4Re$ (480.90): C 34.97, H 2.91, N 2.70; found: C 34.78, H 2.90, N 2.64.

4: Yield: 79%. ^{1}H NMR (300 MHz, $CDCl_3$, 25°C, TMS): $\delta = 13.40$ (s, 1H; NH), 8.60 (s, 1H; CH=N), 7.38–7.36 (m, 2H; Ph), 7.29–7.26 (m, 2H; Ph), 7.03–6.93 (m, 4H; Ph), 3.84 (s, 3H; OCH_3), 2.61 ppm (s, 3H; MTO-CH_3); ^{13}C NMR (100.28 MHz, $CDCl_3$, 25°C): $\delta = 161.41$ (CH=N), 159.89, 158.72, 140.28, 132.84, 131.92, 122.02, 118.96, 118.71, 117.15, 114.47 (aryl-C), 55.29 (Ph-OCH_3), 19.73 ppm (MTO-CH_3); IR (KBr): see Tables 1 and 2; MS (FAB): *m*/*z* (%) 227.9 (100) [M^+−MTO]; elemental analysis calcd (%) for $C_{15}H_{16}NO_5Re$ (476.49): C 37.82, H 3.36, N 2.94; found: C 38.04, H 3.37, N 2.95.

5: Yield: 80%. ^{1}H NMR (300 MHz, $CDCl_3$, 25°C, TMS): $\delta = 13.80$ (s, 1H; NH), 8.59 (s, 1H; CH=N), 7.19 (m, 4H; Ph), 6.97–6.94 (m, 2H; Ph), 6.87 (m, 1H; Ph), 3.91 (Ph-OCH_3), 2.58 (MTO-CH_3), 2.36 ppm (Ph-CH_3); ^{13}C NMR (100.28 MHz, $CDCl_3$, 25°C): $\delta = 161.37$, 151.41, 148.30, 145.11, 136.88, 129.85, 123.52, 120.80, 118.94, 116.25, 114.41, 55.96 (Ph-OCH_3), 20.88 (Ph-CH_3), 19.40 ppm (MTO-CH_3); IR (KBr): see Tables 1 and 2; MS (FAB): *m*/*z* (%) 241.9 (100) [M^+−MTO]; elemental analysis calcd (%) for $C_{16}H_{18}NO_5Re$ (490.51): C 39.18, H 3.70, N 2.86; found: C 39.19, H 3.68, N 2.82.

Single-crystal X-ray structure determination of Complexes 1–5: Details of the X-ray experiment, crystal parameters, data collections and refinements are summarised in Table 8. Single crystals were mounted on a Bruker smart 1000 CCD diffractometer operating at 50 kV and 30 mA equipped with a $Mo_{K\alpha}$ radiation source ($\lambda = 0.71073$ Å). Data collection was performed at 293 K with a ω/ϕ diffraction measurement method and reduction was performed using the SMART and SAINT software with frames of 0.3° oscillation in the θ range $1.5 < \theta < 26.2°$. An empirical absorption correction was applied using the SADABS program. The structures were solved by direct methods and all non-hydrogen atoms were subjected to anisotropic refinement by full-matrix least-squares on F^2 using the SHELXTL package. All hydrogen atoms were generated geometrically (C–H bond lengths fixed at 0.96 Å), assigned appropriate isotropic thermal parameters and included in structure-factor calculations in the final stage of F^2 refinement.[24]

CCDC-609570 (**1**), -609571 (**2**), -609572 (**3**), -609573 (**4**) and -609574 (**5**) contain the supplementary crystallographic data for this paper. These data can be obtained free of charge from the Cambridge Crystallographic Data Centre via www.ccdc.cam.ac.uk/data_request/cif.

Catalytic reactions: *Method A*: *cis*-Cyclooctene (800 mg, 7.3 mmol), 1.00 g of mesitylene (internal standard), H_2O_2 (30% aqueous solution; 1.62 mL, 14.6 mmol) and 1 mol% (73 μmol) of compounds **1**–**5** as catalyst were mixed.

Method B: Styrene (250 mg, 2.39 mmol), 100 mg of mesitylene (internal standard), H_2O_2 (30% aqueous solution; 5.3 mL, 4.78 mmol) and 1 mol% (24 μmol) of compound **3** as catalyst were mixed.

Method C: 1-Octene (800 mg, 7.12 mmol), 1.00 g of mesitylene (internal standard), H_2O_2 (30% aqueous solution; 1.58 mL, 14.2 mmol) and 1 mol% (71 μmol) of compound **3** catalyst were mixed.

Olefin, mesitylene (1 g, internal standard) and compounds **1**–**5** were added to the reaction vessel under air at room temperature and the reaction was started by adding H_2O_2. The course of the reactions was monitored by quantitative GC analysis. Samples were taken at regular time intervals, diluted with CH_2Cl_2, and treated with a catalytic amount of $MgSO_4$ and MnO_2 to remove water and to destroy the unreacted peroxide. The resulting slurry was filtered and the filtrate injected onto a GC column. The conversion of cyclooctene and the formation of cyclooctene oxide were calculated from calibration curves ($r^2 = 0.999$) recorded prior to the reaction.

Acknowledgments

J.Z. thanks the Hochschul- und Wissenschaftsprogramm (HWP-II): Fachprogramm Chancengleichheit für Frauen in Forschung und Lehre for a postdoctoral grant. S.L.Z. and F.E.K. acknowledge the NSFC and the DFG for financial support.

Table 8. X-ray crystal data and data collection and refinement parameters for compunds **1**–**5**.

Compound	**1**	**2**	**3**	**4**	**5**
empirical formula	$C_{14}H_{14}NO_4Re$	$C_{15}H_{16}NO_4Re$	$C_{14}H_{13}ClNO_4Re$	$C_{15}H_{16}NO_5Re$	$C_{16}H_{18}NO_5Re$
formula weight	446.46	460.49	480.90	476.49	490.51
crystal system	monoclinic	monoclinic	monoclinic	monoclinic	triclinic
space group	$P2_1/m$	$P2_1/m$	$P2_1/m$	$P2_1/c$	$P\bar{1}$
a [Å]	9.6219(18)	9.608(3)	9.670(2)	8.9004(16)	7.114(3)
b [Å]	6.7686(13)	6.793(2)	6.8088(15)	16.340(3)	9.494(5)
c [Å]	11.906(2)	12.402(4)	12.428(3)	10.896(2)	11.954(6)
α [°]	90	90	90	90	91.220(7)
β [°]	113.026(3)	109.351(5)	109.125(3)	99.220(3)	90.117(8)
γ [°]	90	90	90	90	94.434(7)
V [Å^3]	713.6(2)	763.7(4)	773.1(3)	1564.1(5)	804.8(7)
Z, ρ_{calcd} [mg m^{-3}]	2, 2.078	2, 2.002	2, 2.066	4, 2.023	2, 2.024
absorption coefficient [mm^{-1}]	8.525	7.969	8.044	7.791	7.574
F(000)	424	440	456	912	472
crystal size [mm^3]	0.30 × 0.26 × 0.20	0.32 × 0.22 × 0.20	0.24 × 0.20 × 0.20	0.32 × 0.28 × 0.24	0.34 × 0.28 × 0.20
θ range for data collection [°]	1.86–26.33	1.74–26.43	1.73–26.35	2.27–26.46	1.70–25.01
reflections collected/unique	4015/1580 [*R*(int) = 0.0597]	4316/1705 [*R*(int) = 0.0439]	4381/1714 [*R*(int) = 0.0518]	8705/3205 [*R*(int) = 0.0485]	3941/2811 [*R*(int) = 0.0376]
goodness-of-fit on F^2	1.058	1.050	1.055	1.019	1.039
final *R* indices [$I > 2\sigma(I)$]					
R_1	0.0433	0.0263	0.0334	0.0368	0.0581
wR_2	0.1034	0.0622	0.0750	0.0764	0.1478
R indices (all data)					
R_1	0.0506	0.0311	0.0474	0.0713	0.0669
wR_2	0.1100	0.0642	0.0816	0.0880	0.1561

[1] I. R. Beattie, P. J. Jones, *Inorg. Chem.* **1979**, *18*, 2318–2319.
[2] a) W. A. Herrmann, J. G. Kuchler, J. K. Felixberger, E. Herdtweck, W. Wagner, *Angew. Chem.* **1988**, *100*, 420–422; *Angew. Chem. Int. Ed. Engl.* **1988**, *27*, 394–396; b) W. A. Herrmann, F. E. Kühn, R. W. Fischer, W. R. Thiel, C. C. Romão, *Inorg. Chem.* **1992**, *31*, 4431–4432; c) W. A. Herrmann, R. M. Kratzer, *Inorg. Synth.* **2002**, *33*, 110–112.
[3] For recent reviews see, for example: a) F. E. Kühn, A. M. Santos, W. A. Herrmann, *Dalton Trans.* **2005**, 2483–2491; b) F. E. Kühn, J. Zhao, W. A. Herrmann, *Tetrahedron: Asymmetry* **2005**, *16*, 3469–3479; c) F. E. Kühn, A. Scherbaum, W. A. Herrmann, *J. Organomet. Chem.* **2004**, *689*, 4149–4164; d) G. Soldaini, *Synlett* **2004**, 1849–1850.
[4] a) W. A. Herrmann, R. W. Fischer, D. W. Marz, *Angew. Chem.* **1991**, *103*, 1704–1706; *Angew. Chem. Int. Ed. Engl.* **1991**, *30*, 1638–1641; b) W. A. Herrmann, R. W. Fischer, W. Scherer, M. U. Rauch, *Angew. Chem.* **1993**, *105*, 1209–1212; *Angew. Chem. Int. Ed. Engl.* **1993**, *32*, 1157–1160; c) A. M. Ajlouni, J. H. Espenson, *J. Am. Chem. Soc.* **1995**, *117*, 9243–9250; d) A. M. Ajlouni, J. H. Espenson, *J. Org. Chem.* **1996**, *61*, 3969–3976; e) F. E. Kühn, A. M. Santos, I. S. Gonçalves, C. C. Romão, A. D. Lopes, *Appl. Organomet. Chem.* **2001**, *15*, 43–50.
[5] a) M. C. A. van Vliet, I. W. C. E. Arends, R. A. Sheldon, *Chem. Commun.* **1999**, 821–822; b) F. E. Kühn, W. A. Herrmann, *Struct. Bonding (Berlin)* **2000**, *97*, 213–236; c) J. Iskara, D. Bonnet-Delpon, J. P. Begue, *Tetrahedron Lett.* **2002**, *43*, 1001–1003; d) R. Buffon, U. Schuchardt, *J. Braz. Chem. Soc.* **2003**, *14*, 347–353; e) R. Saladino, A. A. Andrechi, V. Neri, C. Crestini, *Tetrahedron* **2005**, *61*, 1069–1075; f) E. Da Palma Carreiro, G. Yong-En, A. J. Burke, *J. Mol. Catal. A* **2005**, 2483–2491; g) L. M. Gonzalez, A. L. Vila, C. Montes, G. Gelbard, *React. Funct. Polym.* **2005**, *65*, 169–181; h) D. Ogrin, A. R. Barron, *J. Mol. Catal. A* **2006**, *244*, 267–270; i) S. Gago, J. A. Fernandes, M. Abrantes, F. E. Kühn, P. Ribeiro-Claro, M. Pillinger, T. M. Santos, I. S. Gonçalves, *Microporous Mesoporous Mater.* **2006**, *89*, 284–290.
[6] a) C. C. Romão, F. E. Kühn, W. A. Herrmann, *Chem. Rev.* **1997**, *97*, 3197–3246; b) W. A. Herrmann, F. E. Kühn, *Acc. Chem. Res.* **1997**, *30*, 169–180.
[7] a) W. A. Herrmann, G. Weichselbaumer, E. Herdtweck, *J. Organomet. Chem.* **1989**, *372*, 371–389; b) W. A. Herrmann, J. G. Kuchler, G. Weichselbaumer, E. Herdtweck, P. Kiprof, *J. Organomet. Chem.* **1989**, *372*, 351–370.
[8] a) W. A. Herrmann, R. W. Fischer, M. U. Rauch, W. Scherer, *J. Mol. Catal.* **1994**, *86*, 243–266; b) W. A. Herrmann, F. E. Kühn, M. R. Mattner, G. R. J. Artus, M. Geisberger, J. D. G. Correia, *J. Organomet. Chem.* **1997**, *538*, 203–209; c) W. A. Herrmann, F. E. Kühn, M. U. Rauch, J. D. G. Correia, G. Artus, *Inorg. Chem.* **1995**, *34*, 2914–2920.
[9] a) J. Rudolph, K. L. Reddy, J. P. Chiang, K. B. Sharpless, *J. Am. Chem. Soc.* **1997**, *119*, 6189–6190; b) C. Coperet, H. Adolfsson, K. B. Sharpless, *Chem. Commun.* **1997**, 1565–1566; c) W. A. Herrmann, H. Ding, R. M. Kratzer, F. E. Kühn, J. J. Haider, R. W. Fischer, *J. Organomet. Chem.* **1997**, *549*, 319–322; d) W. A. Herrmann, R. M. Kratzer, H. Ding, W. R. Thiel, H. Glas, *J. Organomet. Chem.* **1998**, *555*, 293–295; e) H. Rudler, J. R. Gregorio, B. Denise, J. M. Bregeault, A. Deloffre, *J. Mol. Catal. A* **1998**, *133*, 255–265; f) H. Adolfsson, A. Converso, K. B. Sharpless, *Tetrahedron Lett.* **1999**, *40*, 3991–3994; g) H. Adolfsson, C. Coperet, J. P. Chiang, A. K. Judin, *J. Org. Chem.* **2000**, *65*, 8651–8658.
[10] a) F. E. Kühn, A. M. Santos, P. W. Roesky, E. Herdtweck, W. Scherer, P. Gisdakis, I. V. Yudanov, C. di Valentin, N. Rösch, *Chem. Eur. J.* **1999**, *5*, 3603–3615; b) P. Ferreira, W. M. Xue, E. Bencze, E. Herdtweck, F. E. Kühn, *Inorg. Chem.* **2001**, *40*, 5834–5842; c) A. M. Santos, F. E. Kühn, K. Bruus-Jensen, I. Lucas, C. C. Romão, E. Herdtweck, *J. Chem. Soc. Dalton Trans.* **2001**, 1332–1337; d) J. Mink, G. Keresztury, A. Stirling, W. A. Herrmann, *Spectrochim. Acta Part A* **1994**, *50*, 2039–2057.
[11] a) M. Nakajima, Y. Sasaki, H. Iwamoto, S. Hashimoto, *Tetrahedron Lett.* **1998**, *39*, 87–88; b) W. D. Wang, J. H. Espenson, *J. Am. Chem. Soc.* **1998**, *120*, 11335–11341; c) C. D. Nunes, M. Pillinger, A. A. Valente, I. S. Gonçalves, J. Rocha, P. Ferreira, F. E. Kühn, *Eur. J. Inorg. Chem.* **2002**, 1100–1107; d) M. J. Sabater, M. E. Domine, A. Corma, *J. Catal.* **2002**, *210*, 192–197; e) E. Da Palma Carreiro, A. J. Burke, M. J. Marcelo Curto, A. J. Teixeira, *J. Mol. Catal. A* **2004**, *217*, 69; f) K. Shimura, K. Fujita, H. Kanai, K. Utani, S. Imamura, *Appl. Catal. A* **2004**, *274*, 253–257; g) J. J. Haider, R. M. Kratzer, W. A. Herrmann, J. Zhao, F. E. Kühn, *J. Organomet. Chem.* **2004**, *689*, 3735–3740; h) S. M. Nabavizadeh, *Dalton Trans.* **2005**, 1644–1648; i) S. M. Nabavizadeh, A. Akbari, M. Rashidi, *Eur. J. Inorg. Chem.* **2005**, 2368–2375; j) S. M. Nabavizadeh, A. Akbari, M. Rashidi, *Dalton Trans.* **2005**, 2423–2427.
[12] W. A. Herrmann, J. D. G. Correia, M. U. Rauch, G. R. J. Artus, F. E. Kühn, *J. Mol. Catal. A* **1997**, *118*, 33–45.
[13] a) P. D. Benny, J. L. Green, H. P. Engelbrecht, C. L. Barnes, S. S. Jurisson, *Inorg. Chem.* **2005**, *44*, 2381–2390, and references therein; b) Z.-K. Li, Y. Li, L. Lei, C.-M. Che, X.-G. Zhou, *Inorg. Chem. Commun.* **2005**, *8*, 307–309; c) W. A. Herrmann, M. U. Rauch, G. R. J. Artus, *Inorg. Chem.* **1996**, *35*, 1988–1991; d) F. E. Kühn, M. U. Rauch, G. M. Lobmaier, G. R. J. Artus, W. A. Herrmann, *Chem. Ber./Recueil* **1997**, *130*, 1427–1431.
[14] W. A. Herrmann, P. Kiprof, K. Rybdal, J. Tremmel, R. Blom, R. Alberto, J. Behm, R. W. Albach, H. Bock, B. Solouki, J. Mink, D. Lichtenberger, N. E. Gruhn, *J. Am. Chem. Soc.* **1991**, *113*, 6527–6537.
[15] a) X. G. Zhou, J. Zhao, A. M. Santos, F. E. Kühn, *Z. Naturforsch. B* **2004**, *59*, 1223–1228; b) J. Zhao, X. G. Zhou, A. M. Santos, E. Herdtweck, C. C. Romão, F. E. Kühn, *Dalton Trans.* **2003**, 3736–3742.
[16] W. A. Herrmann, W. M. Wachter, F. E. Kühn, R. W. Fischer, *J. Organomet. Chem.* **1998**, *553*, 443–452.
[17] W. A. Herrmann, W. A. Wojtczak, G. R. J. Artus, F. E. Kühn, M. R. Mattner, *Inorg. Chem.* **1997**, *36*, 465–471.
[18] W. A. Herrmann, P. W. Roesky, M. Wang, W. Scherer, *Organometallics* **1994**, *13*, 4531–4535.
[19] C. de Méric de Bellefon, W. A. Herrmann, P. Kiprof, C. R. Whitaker, *Organometallics* **1992**, *11*, 1072–1081.
[20] W. A. Herrmann, F. E. Kühn, P. W. Roesky, *J. Organomet. Chem.* **1995**, *485*, 243–251.
[21] M. M. Abu-Omar, P. J. Hansen, J. H. Espenson, *J. Am. Chem. Soc.* **1996**, *118*, 4966–4974.
[22] a) F. E. Kühn, A. M. Santos, M. Abrantes, *Chem. Rev.* **2006**, *106*, 2455; b) C. Freund, M. Abrantes, F. E. Kühn, *J. Organomet. Chem.* **2006**, *691*, 3718.
[23] a) D. R. Lal, S. Keka, *Indian J. Chem. Sect. A* **2000**, *39*, 1177–1181; b) S. Shekhar, K. Abul, *J. Indian Chem. Soc.* **2002**, *79*, 502–504; c) P. P. Singh, B. Srivastava, *Indian J. Chem. Sect. A* **1986**, *25*, 1109–1113.
[24] a) G. M. Sheldrick, SHELXTL97, University of Göttingen, Germany, **1997**; b) SMART V5.618 Software for the CCD Detector System, Bruker Analytical X-ray Systems, Inc., Madison, WI, **1998**; c) SAINTPLUS, V6.45, A Software for the CCD Detector System, Bruker Analytical X-ray System, Inc., Madison, WI, **1998**; d) SADABS V2.10. Program for absorption correction using SMART CCD data based on the method of Blessing: R. H. Blessing, *Acta Crystallogr. Sect. A* **1995**, *A51*, 33.

Received: June 20, 2006
Published online: October 26, 2006

